

**Collision energy dependence of the chemiluminescent reaction:  $\text{Ba} + \text{N}_2\text{O} \rightarrow \text{BaO} + \text{N}_2$**

C. Alcaraz, P. de Pujo, J. Cuvelier, and J. M. Mestdagh

Citation: *The Journal of Chemical Physics* **89**, 1945 (1988); doi: 10.1063/1.455092

View online: <http://dx.doi.org/10.1063/1.455092>

View Table of Contents: <http://scitation.aip.org/content/aip/journal/jcp/89/4?ver=pdfcov>

Published by the **AIP Publishing**

---

**Articles you may be interested in**

Chemiluminescent reactions of electronically excited alkaline earth atoms. II. Energy dependence in  $\text{Ba}^* + \text{O}_2 \rightarrow \text{BaO}^* + \text{O}$

*J. Chem. Phys.* **94**, 4913 (1991); 10.1063/1.460576

Product vibrational distributions and collision energy dependence of chemiluminescent reactions of group IVA elements with  $\text{O}_2$ ,  $\text{N}_2\text{O}$ , and  $\text{NO}_2$

*J. Chem. Phys.* **92**, 4839 (1990); 10.1063/1.457701

Chemiluminescence in reactions of  $\text{N}^+$  ions with hydrogen and hydrocarbons. II. Dependence of total reaction cross sections on the collision energy

*J. Chem. Phys.* **70**, 710 (1979); 10.1063/1.437499

Chemiluminescent reactions of group IIIb atoms with  $\text{O}_2$ : Spectral simulations and extended energy dependence

*J. Chem. Phys.* **69**, 231 (1978); 10.1063/1.436390

HTFFR kinetic studies of the fate of excited  $\text{BaO}$  formed in the  $\text{Ba}/\text{N}_2\text{O}$  chemiluminescent reaction

*J. Chem. Phys.* **66**, 3256 (1977); 10.1063/1.434302

---



# Collision energy dependence of the chemiluminescent reaction: $\text{Ba} + \text{N}_2\text{O} \rightarrow \text{BaO} + \text{N}_2$

C. Alcaraz, P. de Pujo, J. Cuvellier, and J. M. Mestdagh

*Service de Physique des Atomes et des Surfaces, Centre d'Etudes Nucléaires de Saclay,  
91190 Gif-sur-Yvette Cedex, France*

(Received 30 June 1987; accepted 27 April 1988)

The chemiluminescence spectrum of the reaction  $\text{Ba} + \text{N}_2\text{O} \rightarrow \text{BaO} + \text{N}_2$  has been studied using a crossed beam apparatus as a function of the collision energy over the range 0.1–0.6 eV. The relative importance of its red wing increases as the collision energy is raised. Moreover, the cross section associated to chemiluminescence at a wavelength  $\lambda$  of the range 450–700 nm goes through a maximum as the collision energy is varied, the position of which depends significantly on the value of  $\lambda$ . The importance of this effect cast some doubt about works, where the energy dependence of the “total” chemiluminescence is measured using a detector which does not have a constant response over the wide range of the chemiluminescence. The analysis of the present results reveals that increasing the collision energy results in lowering the average vibrational excitation present in the emitting states  $A\ ^1\Sigma^+$  and  $A'\ ^1\Pi$  of the product BaO.

## I. INTRODUCTION

Since the first study of its chemiluminescent channel by Ottinger and Zare,<sup>1</sup> many aspects of the reaction

$\text{Ba} + \text{N}_2\text{O} \rightarrow \text{BaO} + \text{N}_2$ ,  $\Delta H_0^\circ = 4.11 \pm 0.09$  eV (1)  
have been studied.<sup>2–4</sup> Regarding the chemiluminescent channel



and those experiments performed under single collision conditions, Jalink *et al.* have pointed out that a complete analysis of the chemiluminescence spectrum and a mechanism which accounts for the main features of process (2) are not yet available.<sup>4,5</sup> This motivates for further investigations of this process.

The total chemiluminescence signal resulting in process (2) has been studied as a function of the collision energy under single collision conditions.<sup>4,6,7</sup> The signal peaks near 0.16 eV, and decreases regularly at higher energies.<sup>4,6,7</sup> Reference 7 claims that within the experimental uncertainties, the shape of the chemiluminescent spectrum is not affected by varying the collision energy over the range 0.1–0.8 eV. This observation is at odds with a more recent work.<sup>5</sup> Reference 5 is essentially concerned with process (2) for reactions of spatially oriented  $\text{N}_2\text{O}$ , but it is shown also that for reactions of randomly oriented molecules, the chemiluminescence spectrum shifts slightly to the red as the collision energy is increased between 0.105 and 0.162 eV. If confirmed, such a distortion of the spectrum certainly contains useful information on the mechanism responsible for branching to the chemiluminescence channel in  $\text{Ba} + \text{N}_2\text{O}$  collisions.

Two such mechanisms have been proposed so far. Field *et al.*<sup>8</sup> have suggested that the perturbations of the BaO states due to the large rotation of BaO resulting from the  $\text{Ba} + \text{N}_2\text{O}$  reaction favor a rotational coupling between the predominantly populated ground state  $\text{BaO}(X\ ^1\Sigma^+)$  and the emitting states  $A\ ^1\Sigma^+$  and  $A'\ ^1\Pi$ . Since much scrambling of these states occurs, the distinction between  $A\ ^1\Sigma^+$  and

$A'\ ^1\Pi$  may vanish. In contrast, Jalink *et al.* have proposed that couplings due to departure of  $\text{N}_2$  could be the ones which turn on the chemiluminescence.<sup>4</sup> In both cases, the mechanisms are dynamical models that have been proposed as qualitative interpretations of experimental observations: population of the vibrational levels of the emitting states in the first case, energy dependence of the total chemiluminescence for state selected  $\text{N}_2\text{O}$  molecules in the second case.

This paper reports on a crossed beams investigation of process (2), where the shape of the chemiluminescence spectrum is studied as a function of the collision energy over a wide range. Since the collision energy is the essential dynamical parameter of a collision, it is hoped that the present work will bring a useful quantitative basis to further discussions of the above cited models when the couplings they involve will be calculated theoretically.

## II. EXPERIMENTAL

A supersonic  $\text{N}_2\text{O}$  beam seeded with He is crossed at right angles with a weakly supersonic Ba beam generated from a 800 °C heated oven. This arrangement has been described elsewhere.<sup>9</sup> The control and measurement devices, however, need to be presented in more details.

### A. Beam fluxes and collision energy

The Ba flux is monitored by a hot-wire detector. The  $\text{N}_2\text{O}/\text{He}$  flux is measured using a tandem Pitot tube + mass spectrometer. The pressure difference in the Pitot tube chamber whether the  $\text{N}_2\text{O}/\text{He}$  beam is on and off gives the total flux  $\text{He} + \text{N}_2\text{O}$  of the beam. The mass spectrometer is sitting at the end of a time-of-flight path, when tuned to the mass of He, it allows one to extract the contribution of He from the Pitot tube signal, and thus to deduce the  $\text{N}_2\text{O}$  flux in the beam.

The collision energy is varied between 0.10 and 0.20 eV, by changing the  $\text{N}_2\text{O}/\text{He}$  mixture. The stagnation chamber generating the  $\text{N}_2\text{O}/\text{He}$  beam is then operating at room tem-

perature. When this chamber is kept at 470 K, still operating with the  $\text{N}_2\text{O}/\text{He}$  mixture, the 0.15–0.60 eV energy range is covered. The  $\text{N}_2\text{O}$  velocity and the corresponding velocity distribution are measured using the time-of-flight technique. The full width at half maximum of the collision energy distribution varies from 0.07 to 0.17 eV for collision energies ranging between 0.10 and 0.60 eV.

### B. Fluorescence measurement devices

The scattering region is imaged onto the entrance slit of a monochromator. The essential difference between the apparatus used here and that described in Ref. 9 is a substantially improved sensitivity of the optical system for collecting the light emitted in the scattering region. Since structureless chemiluminescence spectra are expected,<sup>3</sup> a wavelength resolution limit of 8 nm was chosen on the monochromator. The chemiluminescence signal is detected using a photomultiplier RCA31034.

The scattering zone is also imaged onto a second RCA31034 photomultiplier in order to record the undispersed chemiluminescence. To prevent the photomultiplier to be blind by the red thermal radiation of the Ba source, a 1 mm Schott-BG39 color filter is placed in front of it. In experiments at fixed collision energies, this secondary measurement allows one to monitor the fluctuations of the reactant beams over large time scales. This secondary measurement also provides useful comparisons with the existing literature.

### C. Characterization of the molecular beam

Under a 470 K stagnation temperature, which is our largest operating temperature, about 17% of the  $\text{N}_2\text{O}$  molecules are vibrationally excited to the level  $v_2 = 1$  of the bending mode. This fraction is much lower in the beam because of the intense cooling resulting from the supersonic expansion. The stagnation pressure  $p_0$  in the chamber generating the  $\text{N}_2\text{O}$  beam is fixed to 760 Torr or more, and the nozzle diameter  $d$  to 0.2 mm. This gives the product  $p_0 \cdot d$  a large value which ensures a significant cooling of the bending mode in the expansion. As a result, the present results essentially reflect the reactivity of  $\text{N}_2\text{O}(v_2 = 0)$  with Ba. We shall come back to this point in Sec. III. The rotational temperature of  $\text{N}_2\text{O}$  in the beam is below 50 K.

The  $\text{N}_2\text{O}/\text{He}$  beam is operating with no  $\text{N}_2\text{O}$  cluster present. This has been checked by first looking to the absence of dimers and higher polymers in the beam mass spectrum, and second by analyzing the velocity distribution of the beam particles with the mass spectrometer tuned to the mass of  $\text{N}_2\text{O}$ . We have shown indeed in a previous work that the formation of large clusters during the supersonic expansion shows up as a bimodal shape of the monomer time-of-flight signal.<sup>10</sup> The requirement of no cluster present in the beam necessitates a careful choice of the stagnation pressure, the stagnation temperature, and the  $\text{N}_2\text{O}/\text{He}$  mixture. As a result, the choice of the collision energy is less flexible than desired.

### D. Experimental procedures

Two types of experiments are performed:

(i) Chemiluminescence spectra are recorded for two collision energies, 0.15 and 0.60 eV: the monochromator is scanned over the spectral range 415–900 nm and the corresponding signal is recorded using a multichannel scale.

(ii) The chemiluminescence signal  $I(\lambda, E)$  is measured as a function of the collision energy  $E$  over the range 0.10–0.60 eV with the monochromator sitting at various wavelengths  $\lambda$ , 450, 500, 600, and 700 nm.  $I(\lambda, E)$  is recorded simultaneously with the undispersed chemiluminescence using counting scales. This procedure is more accurate than the first one. The signals, indeed, are accumulated over a long time, and the uncertainties on  $I(\lambda, E)$  due to long time scale fluctuations of the reactant beams can be determined using the measurement of the total chemiluminescence.

### III. RESULTS

The chemiluminescence spectra recorded using the experimental procedure (i) of Sec. II D at the collision energies 0.15 and 0.60 eV are shown in Fig. 1 over the spectral range 415–805 nm. The peak of each spectrum is normalized to unity. Above 805 nm, the signal that has been recorded separately is very weak and is not reported here. It decreases smoothly down to the extinction.

The spectrum at 0.15 eV collision energy is qualitatively similar to those of the literature obtained under single collision conditions at comparable energies.<sup>1,3,5,11</sup> Quantitative comparisons are impossible, however, since (i) the spectra of Ref. 3 were obtained under beam-gas conditions, i.e., with different reactant internal energies, (ii) those of Refs. 1 and 11 were not corrected for the detector transmission, and that

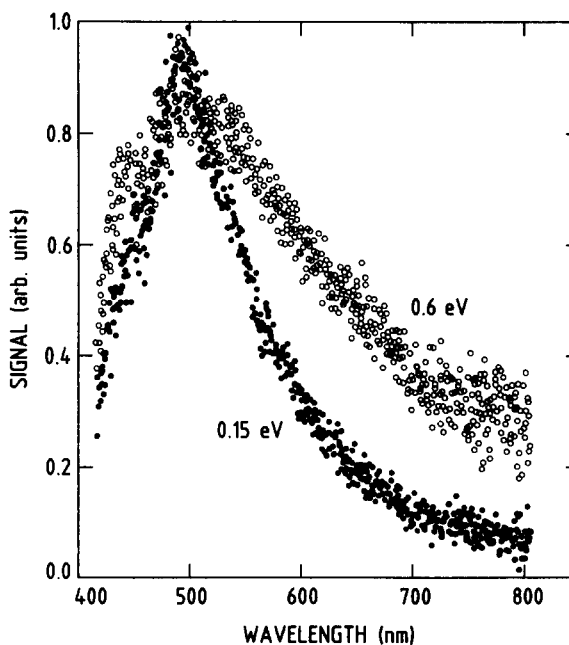


FIG. 1. Chemiluminescence spectrum from the  $\text{Ba} + \text{N}_2\text{O}$  reaction at collision energies of 0.15 (full circles) and 0.6 eV (open circles). The spectra are corrected for the transmission and detection efficiencies.

of Ref. 5 was obtained with a too low wavelength resolution. As expected, the spectra of Fig. 1 are structureless, indicating a substantial rotational excitation of BaO.

The new information brought by Fig. 1 is the change in the chemiluminescence spectrum as the collision energy switches from 0.15 to 0.6 eV. The chemiluminescence red wing is reinforced as the collision energy is increased. In contrast, the blue wing remains fairly constant. These results are consistent with those of Ref. 5 obtained over the limited energy range 0.105–0.162 eV.

The experimental procedure (ii) of Sec. II D allows one to measure the cross section  $\sigma(\lambda, E)$  of process (2) in relative values for a given chemiluminescence wavelength  $\lambda$  as a function of the collision energy  $E$ . It is given by

$$\sigma(\lambda, E) = \alpha \cdot I(\lambda, E) / [n(\text{N}_2\text{O}) \cdot V], \quad (3)$$

where  $I(\lambda, E)$  is the chemiluminescence intensity,  $n(\text{N}_2\text{O})$  is the  $\text{N}_2\text{O}$  density as deduced from the Pitot tube + mass spectrometer measurement, and  $V$  is the relative velocity of Ba and  $\text{N}_2\text{O}$  as deduced from the time-of-flight measurement.  $\alpha$  is a proportionality constant.

The results are shown in Fig. 2: the cross section ratio  $\sigma(\lambda, E)/\sigma(\lambda, 0.10 \text{ eV})$  is plotted as a function of the collision energy over the range 0.10–0.60 eV, for four wavelengths  $\lambda = 450, 500, 600,$  and  $700 \text{ nm}$ . The relative value of the cross section  $\sigma(\lambda, E)$  first increases with the collision energy, and then decreases. The interesting point revealed by Fig. 2 is that the maximum shifts to larger collision energies as the wavelength  $\lambda$  goes to the red: it is between 0.1 and 0.15 eV for 450 nm, and at about 0.3 eV for 700 nm.

As said in the Sec. II, a side measurement of the present work is the total chemiluminescence resulting in process (2) as a function of the collision energy. The corresponding cross section is plotted in Fig. 3. It goes through a maximum

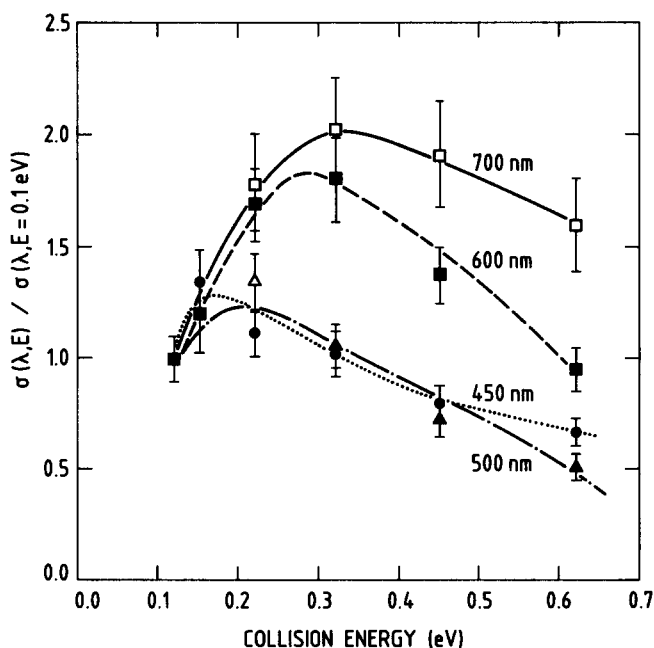


FIG. 2. Collision energy dependence of the cross section ratio  $\sigma(\lambda, E)/\sigma(\lambda, 0.10 \text{ eV})$  for four values of the chemiluminescence wavelength  $\lambda = 450$  (circles),  $500$  (triangles),  $600$  (full squares), and  $700 \text{ nm}$  (open squares). The curves are just for guiding the eyes.

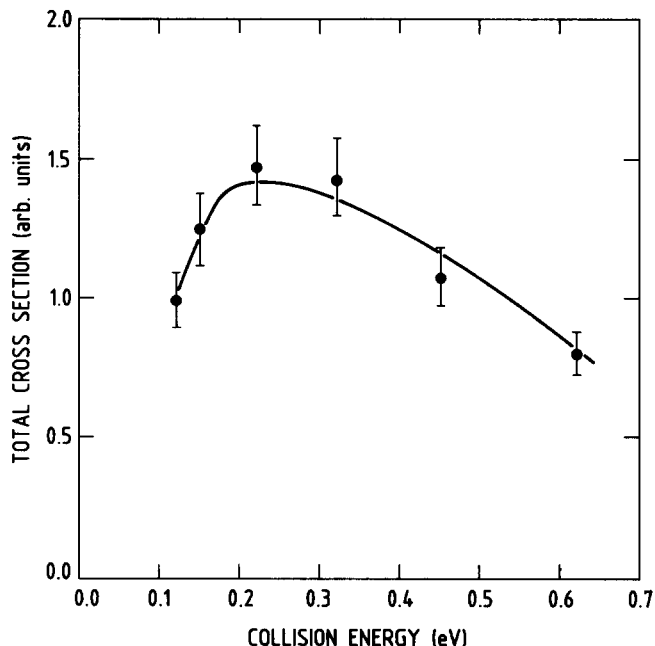


FIG. 3. Collision energy dependence of the total chemiluminescence cross section. The solid curve is just for guiding the eyes. See the text for the cautions regarding this figure.

near 0.2 eV collision energy. Qualitatively, it looks very much like that of Refs. 6 and 7, where the  $\text{N}_2\text{O}$  was vibrationally cold, and that of Ref. 4 where  $\text{N}_2\text{O}$  was state selected to the lowest level  $v_2 = 0$  of the bending mode. This result is expected since in our experiment, the  $\text{N}_2\text{O}$  bending mode is intensively cooled by the supersonic expansion.

It is worthwhile to consider Fig. 3 in more detail, and to outline that in this experiment, as well as in those of Refs. 4, 6, and 7, the measured “total” chemiluminescence is the true one convoluted by the response of the fluorescence detector. In our case, this response is maximum at 500 nm, and is half of the maximum at 600 nm. In contrast, the efficiency of the detector used in Ref. 4 is maximum at 400 nm, and goes to zero at 600 nm, due to the bialkali photocathode of the photomultiplier. The fluorescence detected in Ref. 4, thus corresponds to a bluer part of the total chemiluminescence than in our experiment. This introduces a bias in the measured energy dependence since the blue wing and the red wing of the spectrum do not have the same energy dependence (see Fig. 2). This explains why the maximum of the cross section of Fig. 3 is at slightly larger collision energies than the corresponding one of Ref. 4 (about 0.2 against 0.16 eV).

The last point should make the reader very careful when considering the collision energy dependence of the undispersed chemiluminescence of process (2), such as that given in Fig. 3 of the present work or that given in Refs. 4, 6, and 7. In particular, the results of Fig. 2 must be recommended over those of Fig. 3, even when apparently, only information on the total chemiluminescence is needed.

#### IV. DISCUSSION

Let us first consider the spectra of Fig. 1. To help in discussing their relative shape, Fig. 4 shows the vibrational

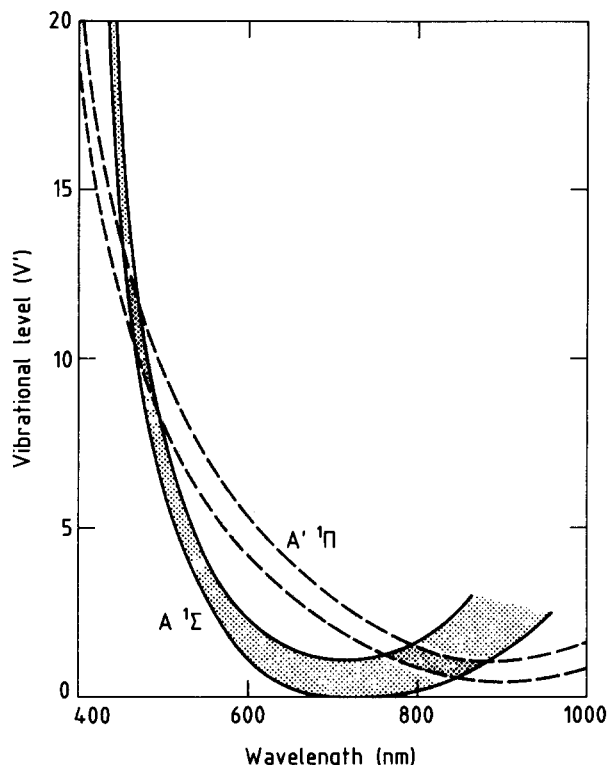


FIG. 4. The ordinate of the figure gives the range of vibrational levels  $v'$  of  $\text{BaO}(A' {}^1\Sigma^+)$  and  $\text{BaO}(A' {}^1\Pi)$  which have the largest Franck-Condon factors for fluorescence emission at the wavelengths given on the abscissa of the figure.

levels  $v'$  of the excited states  $\text{BaO}(A' {}^1\Sigma^+)$  and  $A' {}^1\Pi$  which have the largest Franck-Condon factors for fluorescence emission at a given wavelength  $\lambda$ . The states  $A' {}^1\Sigma^+$  and  $A' {}^1\Pi$  are those responsible for the observed chemiluminescence. It is readily apparent in Fig. 4 that the range 400 to 500 nm essentially corresponds to fairly large vibrational quantum numbers of the emitting molecule ( $v' \geq 8$ ), and that wavelengths between 600 and 800 nm are emitted by molecules of low vibrational excitation ( $v' \leq 3$ ).

The two spectra of Fig. 1 peak around 500 nm. According to Fig. 4, this indicates that at both energies the electronically excited BaO has a substantial vibrational population around  $v' = 10$ . A second observation in Fig. 1 is that the spectrum red wing is enhanced as the collision energy switches from 0.15 to 0.6 eV. This suggests that at 0.6 eV, small vibrational quantum numbers of BaO are more populated than at 0.15 eV. The following picture thus emerges: the vibrational distribution of the emitting state peaks around  $v' = 10$  at 0.15 eV collision energy, and at 0.6 eV it broadens out towards lower values of  $v'$ . This picture is the same whatever the emitting states,  $A' {}^1\Sigma^+$  or  $A' {}^1\Pi$ .

A numerical simulation of the BaO chemiluminescence, using assumed vibrational distributions of the emitting state  $A' {}^1\Pi$  or  $A' {}^1\Sigma^+$  is useful to substantiate the picture drawn above. The simulation section of the SIML code of Ref. 12 is used for this purpose. Sample vibrational distributions which lead to a good fit of the spectra of Fig. 1 are shown in Fig. 5. They correspond to  $\text{BaO}(A' {}^1\Sigma^+)$  as emitter. They nicely confirm the qualitative picture drawn in the previous

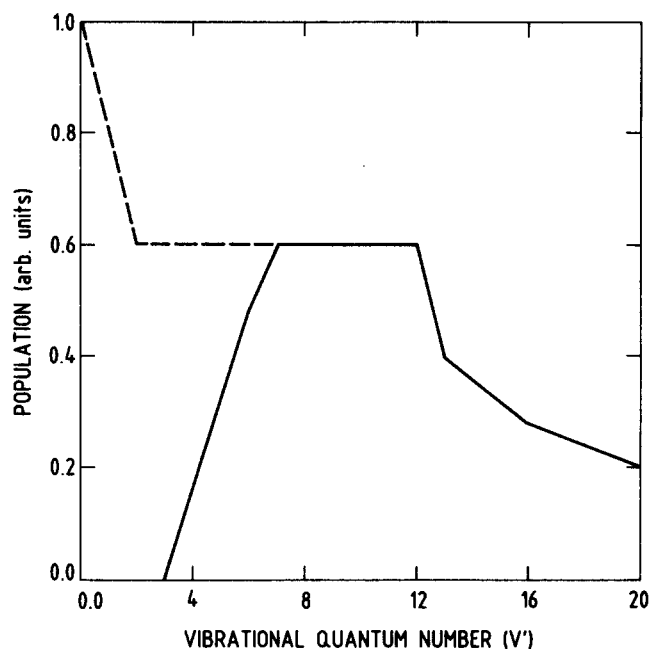


FIG. 5. Vibrational distribution of the  $A$  state corresponding to a good fit of the experimental chemiluminescence spectra of Fig. 1. The full curve corresponds to 0.15 eV collision energy, and the dashed curve to 0.6 eV. Above  $v' = 7$  both curves are running together.

paragraph. Calculations performed using  $A' {}^1\Pi$  as emitter lead to similar conclusions.

Additionally, the above simulations allow one to give a lower limit of the BaO rotational excitation. Taking into account the spectral resolution of the measurement, a rotational temperature higher than 4000 K is required to reproduce the observation of Fig. 1 where no band structure is visible.

Let us discuss the results of Fig. 2 further. The cross section peaks at larger collision energies as the observation wavelength is increased. This result can be rationalized easily when considering that the increase of the collision energy above 0.2 eV has two opposite effects on the chemiluminescence: firstly, the total chemiluminescence decreases as shown in Refs. 4, 6, and 7 and in Fig. 3, and secondly, the chemiluminescence at 600–700 nm is enhanced with respect to that at 450–500 nm as observed in the present work. According to this, Fig. 2 tells that the relative enhancement of the chemiluminescence in the red compensates the general decrease of the total cross section up to energies of 0.25 eV at 600 nm and 0.35 eV at 700 nm.

Finally, it is worthwhile to bring the present results concerning the chemiluminescent channel together with results regarding the nonchemiluminescent channel of the  $\text{Ba} + \text{N}_2\text{O}$  reaction. An increase in the collision energy results in a decrease of the internal excitation present in the reaction products BaO and  $\text{N}_2$  for the nonchemiluminescent channel.<sup>13</sup> This decrease is certainly shared between the two products. It is thus consistent to conclude that the  $\text{BaO}(X' {}^1\Sigma^+)$  vibrational excitation decreases as the collision energy is increased. This behavior is the same as that observed in the present work for the chemiluminescent channel forming  $\text{BaO}(A' {}^1\Sigma^+, A' {}^1\Pi)$ . This suggests either

that a unique reaction mechanism leads directly to both the chemiluminescent and the nonchemiluminescent channels, or that the chemiluminescence is indirectly coming from the nonchemiluminescent reaction through couplings at late stages of the collision. The models of Field *et al.*,<sup>8</sup> and Jalink *et al.*<sup>4</sup> recalled in Sec. I, both follow this picture. However the lack of quantitative information concerning the couplings they involve prevent decision as to which one is the most promising to account for the  $\text{Ba} + \text{N}_2\text{O}$  reaction.

## V. CONCLUSION

The chemiluminescence spectrum resulting from  $\text{Ba} + \text{N}_2\text{O}$  reactions has been studied as a function of the collision energy over the range 0.10–0.60 eV. The experiments are performed under a single collision regime using a crossed beam apparatus. The spectrum is structureless at all the energies studied, whereas the spectrum envelope is energy dependent. Increasing the collision energy results in enhancing the spectrum red wing with respect to the blue wing. These observations indicate that the average vibrational excitation of the emitting states  $A^1\Sigma^+$  or  $A'^1\Pi$  of BaO decreases as the collision energy is raised.

The cross section corresponding to chemiluminescence at a given wavelength  $\lambda$  of the range 450–700 nm has also been measured as a function of the collision energy. It goes through a maximum which is located at larger energies for larger values of  $\lambda$  (e.g., 0.15–0.2 eV at 450 nm vs 0.3 eV at 700 nm). This was interpreted as a compensation between the enhanced relative importance of the spectrum red wing and the general lowering of the chemiluminescence cross section when the collision energy is increased. Since the collision energy dependence of the chemiluminescence cross section depends significantly on the chemiluminescence wavelength, some doubt can be cast on works where the energy dependence of the “total” chemiluminescence is mea-

sured using a detector which does not have a constant response over the wide range of the chemiluminescence.

These results offer a quantitative basis to check the models that have been proposed in the literature to account for the chemiluminescent channel in  $\text{Ba} + \text{N}_2\text{O}$  reactions. However, this requires quantitative information on the coupling mechanisms involved in these models that is not currently available. It is thus hoped that the present results will motivate theoretical works to answer this question.

## ACKNOWLEDGMENTS

The authors are grateful to A. Binet and P. Meynadier for their assistance with the experimental work, and to J. Berlande and J.P. Visticot for valuable discussions.

<sup>1</sup>C. Ottinger and R. N. Zare, *Chem. Phys. Lett.* **5**, 243 (1970).

<sup>2</sup>J. J. Reuther and H. B. Palmer, *J. Chem. Phys.* **77**, 83 (1982).

<sup>3</sup>J. W. Cox and P. G. Dagdigan, *J. Chem. Phys.* **79**, 5351 (1983).

<sup>4</sup>H. Jalink, F. Harren, D. Van Den Ende, and S. Stolte, *Chem. Phys.* **108**, 391 (1986).

<sup>5</sup>H. Jalink, S. Stolte, and D. H. Parker, *Chem. Phys. Lett.* **140**, 215 (1987).

<sup>6</sup>D. J. Wren and M. Menzinger, *J. Chem. Phys.* **63**, 4557 (1975).

<sup>7</sup>D. J. Wren and M. Menzinger, *Faraday Discuss. Chem. Soc.* **67**, 97 (1979).

<sup>8</sup>R. W. Field, R. A. Gottscho, J. G. Pruett, and J. J. Reuther, in *Proceeding of the 14th International Symposium of Free Radicals* (Association for Science Documents Information, Japan, 1979), pp. 39–59.

<sup>9</sup>J. Cuvelier, J. M. Mestdagh, J. Berlande, P. de Pujo, and A. Binet, *Rev. Phys. Appl.* **16**, 679 (1981); J. M. Mestdagh, J. Berlande, J. Cuvelier, P. de Pujo, and A. Binet, *J. Phys. B* **15**, 439 (1982).

<sup>10</sup>J. Cuvelier and J. Binet, *Rev. Phys. Appl.* **23**, 91 (1988).

<sup>11</sup>L. Nanquan and Z. Xiankang, *Sci. Sin.* **26**, 126 (1983).

<sup>12</sup>M. Prisant and R. N. Zare, in *Gas Phase Chemiluminescence and Chemiionization*, edited by A. Fontijn (North-Holland, Amsterdam, 1985), p. 189; *J. Chem. Phys.* **83**, 5458 (1985).

<sup>13</sup>T. P. Parr, A. Freedman, R. Behrens, Jr., and R. R. Herm, *J. Chem. Phys.* **67**, 2181 (1977).